atmosphere

MDPI

Article

Spatiotemporal Precipitation Trends and Associated Large-Scale Teleconnections in Northern Pakistan

Ansa Rebi [1,2,†], Azfar Hussain [3,†], Ishtiaq Hussain [4], Jianhua Cao [3], Waheed Ullah [5], Haider Abbas [6], Safi Ullah [7] and Jinxing Zhou [1,2,*]

[1] Jianshui Research Station, School of Soil and Water Conservation, Beijing Forestry University, Beijing 100083, China; ansarebi@bjfu.edu.cn
[2] Key Laboratory of State Forestry and Grassland Administration on Soil and Water Conservation, Beijing Forestry University, Beijing 100083, China
[3] International Research Center on Karst under the Auspices of UNESCO, Institute of Karst Geology, Chinese Academy of Geological Sciences, Guilin 541004, China; azfarhussayn@gmail.com (A.H.); jhcaogl@karst.ac.cn (J.C.)
[4] Department of Applied Mathematics, Chung Yuan Christian University, Taoyuan 32023, Taiwan; ishtiaqhucane@gmail.com
[5] Defense and Security, Rabdan Academy, Abu Dhabi 114646, United Arab Emirates; wullah@ra.ac.ae
[6] Synthesis Research Centre of Chinese Ecosystem Research Network, Key Laboratory of Ecosystem Network Observation and Modelling, Institute of Geographic Sciences and Natural Resources Research, Chinese Academy of Sciences, Beijing 100101, China; habbas@igsnrr.ac.cn
[7] Department of Atmospheric and Oceanic Sciences, Institute of Atmospheric Sciences, Fudan University, Shanghai 200433, China; safikhalil442@yahoo.com
* Correspondence: zjx001@bjfu.edu.cn
† These authors contributed equally to this work.

Abstract: The effects of climate change are unparalleled in magnitude, ranging from changing weather patterns that endanger food production to increasing sea levels that increase the likelihood of catastrophic flooding. Therefore, determining the extent of such variations on regional and local scales is imperative. We used monthly precipitation data from 25 meteorological stations in northern Pakistan (NP) to document the observed changes in seasonal and annual precipitation. The station density in the NP is small and unevenly distributed; therefore, ERA-5 reanalysis data were used to supplement the observed dataset to assess the spatial trends in NP. The non-parametric Mann–Kendall (MK), Sen's Slope estimator (SSE), and Sequential Mann–Kendall (SQMK) tests were performed to assess the trends. In addition, the wavelet analysis technique was used to determine the association of precipitation with various oceanic indices from 1960 to 2016. Results indicate that maximum precipitation was shown in the annual and summer seasons. In NP, annual, winter, spring, and summer precipitation declined, while an increase in autumn was observed at a rate of 0.43 mm/decade between 1989 and 2016. The spatial trends for observed and ERA-5 reanalysis datasets were almost similar in winter, spring, and autumn; however, some disagreement was observed in both datasets in the summer and annual precipitation trends in NP during 1960–2016. Between 1989 and 2016, summer and annual precipitation increased significantly in Region III. However, seasonal and annual precipitation decreased in NP between 1960 and 2016. Moreover, there were no prominent trends in annual precipitation until the mid-1980s, but an apparent increase from 1985 onwards. Annual precipitation increased in all elevations except at the 500–1000 m zone. The ENSO (El Niño–Southern Oscillation) shared notable interannual coherences among all indices above 16–64 months. Inter-decadal coherence with the ENSO, AO (Arctic Oscillation), and PDO (Pacific Decadal Oscillation) in NP for 128 months and above. Generally, AO, AMO (Atlantic Multidecadal Oscillation), and NAO (North Atlantic Oscillation) exhibited less coherence with precipitation in NP. The regression of seasonal and annual precipitation revealed that winter and spring precipitation levels had higher linear regression with the AO and ENSO, respectively, while both the AO and ENSO also dominated at the annual scale. Similarly, the IOD and PDO indices had a higher influence in summer precipitation. The findings may help water resource managers and climate researchers

Citation: Rebi, A.; Hussain, A.; Hussain, I.; Cao, J.; Ullah, W.; Abbas, H.; Ullah, S.; Zhou, J. Spatiotemporal Precipitation Trends and Associated Large-Scale Teleconnections in Northern Pakistan. *Atmosphere* **2023**, *14*, 871. https://doi.org/10.3390/atmos14050871

Academic Editors: Nicole Mölders and Mario Marcello Miglietta

Received: 7 March 2023
Revised: 1 May 2023
Accepted: 11 May 2023
Published: 15 May 2023

develop a contingency plan for better water resource management policies in the face of changing climate change in Pakistan, particularly in NP.

Keywords: precipitation; cluster analysis; wavelet coherence; oceanic indices; northern Pakistan

1. Introduction

Precipitation is an essential variable that significantly impacts the global climate system and energy cycle [1], i.e., hydrological, ecological, and biochemical processes [2]. Global warming directly influences the spatial and temporal variability of precipitation [3]. Climate variability in different climate zones varies due to substantial variances in the climatic backdrop, various driving forces, and regional peculiarities [4,5]. So, having good knowledge of precipitation amounts that reach the land surface is crucial to assess fresh water and manage hydrology, agriculture, and land use, including flood and drought risk [6–8]. Therefore, quantifying the trends and variabilities in precipitation on a regional scale is of paramount concern [4,9].

Due to the complex topography, dynamic climatology, and inadequate coping capacity, Pakistan is one of the most vulnerable countries to climate change [10,11]. It is among the top ten countries most affected by extreme climate events [12,13]. Climate change has significantly affected the spatiotemporal variability of precipitation in Pakistan [14]. This variability affects the availability of water resources, resulting in hydrometeorological disasters in the country [15,16]. Recent floods (in 2010) and prolonged drought (from 1997 to 2002) are examples of climate-related extremes that affected millions of people nationwide. The northern highlands of Pakistan are prone to floods [17], whereas the southern areas are drought-prone [18].

Numerous previous studies have highlighted the dynamic variability of precipitation in different parts of Pakistan. For example, Hartman (2012) reported a decreasing trend of precipitation in the western part of the Indus Basin and an increasing trend in the northern and eastern parts [19]. Similarly, increasing seasonal and annual precipitation trends were observed in the Upper Indus Basin (UIB) [20]. An increase in annual precipitation in the Himalayan region was reported by Adnan et al. [21] and Gadiwala et al. [22]. An annual and significant seasonal increase was observed in the Swat Basin [23].

Considering the association of global teleconnections with precipitation in northern Pakistan (NP), Iqbal and Hussain [24] explored the influence of ocean–atmospheric circulations on precipitation during 1976–2013 and observed that the NAO, ENSO, and PDO influenced precipitation in the Azad Jammu and Kashmir, while the IOD, ENSO, and NAO influenced precipitation in Khyber Pakhtunkhwa. Afzal et al. [25] investigated the influence of the NAO and ENSO on winter precipitation in NP and found that the NAO is less influential than the ENSO, and they observed that precipitation remained normal in this region with the positive phase of the NAO and the negative phase of the ENSO. Hussain et al. [20] examined precipitation variation and the influence of climate indices on precipitation in the UIB and observed that the PDO showed less significant results. In contrast, the ENSO showed significant results compared to the NAO and IOD. The combined interaction of the Pacific Ocean and the atmosphere affects the strength and location of the westerly jet, which gives shape to the western disturbance via teleconnection that intrudes Pakistan from the west [26]. According to Lau and Kim [17], the Russian heatwave was due to the blocking of extratropical atmospheric events linked with atmospheric Rossby wave trains over central Asia and the Tibetan Plateau.

After a detailed literature review on variability, trends, and teleconnections, the region needs a more intensive and organized analysis of precipitation variations over its various homogenous climatic regions and their associations with large-scale oceanic indices. Whether NP's seasonal and annual precipitation trends are changing due to climate change needs detailed and systematic evaluation. Furthermore, there have been few investigations

on the effects of precipitation variation in this region [19,27]. Despite the significant impact of climate change on precipitation patterns and associated consequences for water resource management and agriculture in northern Pakistan, there is a lack of research on the spatiotemporal trends of precipitation over homogenous climatic regions and their relationship with large-scale mechanisms. Previous studies have focused on the overall precipitation trends without considering the homogenous regions, which may provide valuable insights for effective water resource planning and management. Additionally, few studies have explored the potential links between precipitation trends in northern Pakistan and large-scale influencing mechanisms, such as the El Niño–Southern Oscillation (ENSO) and the Indian Ocean Dipole (IOD), which are known for their significant influence on the regional climate. Therefore, this study aims (1) to identify the homogenous precipitation regions using cluster analysis, (2) to assess the spatial and temporal trend of seasonal and annual precipitation from 1960 to 2016, and (3) to investigate the association between large-scale climate indices, i.e., the AMO, AO, NAO, ENSO, PDO, and PNA. The findings of this study could help water resource managers and climate scientists to develop a contingency plan for better water resource management in the face of changing climate change.

2. Study Area

Pakistan has a subtropical to tropical climate, with a latitudinal range of 23 to 37 degrees north and a longitudinal span of 61 to 78 degrees east [28]. The highest elevation is about 8611 m, which is of the world's second-highest mountain (K-2) [20]. The geography of Pakistan is diverse, having high peaks in the upper reaches, flat agricultural terrain in the middle, and a coastal belt in the lower reaches [29]. Pakistan's total mean annual precipitation is 481 mm [30]. NP's primary precipitation sources are monsoon winds and western disturbances [31]. Western disturbances originating from the Mediterranean region bring winter precipitation to NP [32,33], whereas monsoon winds arise from the Indian Ocean and the Bay of Bengal due to the difference in temperature between land and ocean. Precipitation is abundant in the NP, including upper Khyber Pakhtunkhwa (KPK) and Kashmir [34]. It plays a crucial role in agricultural and economic activities in Pakistan [35]. Agriculture is primarily climate-dependent, with each region having its crops and fruits suited to its climate [36,37]. The country's most important crops and fruits are cultivated in the summer season in various places depending on the environment [38].

3. Materials and Methods

3.1. Dataset and Preprocessing

The Pakistan Metrological Department (PMD) provides monthly precipitation data from 1960 to 2016 (Figure 1 and Table 1). These stations are not evenly distributed all over NP, and the number of stations covering this region is very small. Therefore, we also used ERA-5 reanalysis data along with the station data to assess the precipitation trends in the whole region for the study period. ERA-5 precipitation datasets can be used as an alternative to observed data due to their better performance [39]. The PMD collects, compiles, and screens all metrological variables to ensure quality. A standardized normal homogeneity test (SNHT) approach was used for homogeneity testing [40]. This approach was used to decrease the influence of non-climatic factors on climate series [41,42]. The relative and standalone tests were also used for this purpose. Autocorrelation analysis was applied in precipitation time series to remove any autocorrelation before trend analysis [43–46], as autocorrelation affects the trend results. Autocorrelation values were calculated with a 95% confidence interval for precipitation data. A flow chart of the data pre-processing, methodology, and analysis is shown in Figure 2. It should be noted that the datasets used in the study have limitations in terms of spatial scales. The area did not have enough ground-based observations over the whole region with a uniform distribution, while it only covers NP, which may not be representative of precipitation trends in other regions. The numbers of meteorological stations in the sub-regions I–III are 11, 10, and 4, respectively (Table 2). The locations of each homogenous region in Pakistan are R-I (Gilgit-Baltistan and Chitral

region, Upper Indus Basin and Chitral River Basin, Hindukush–Karakoram–Himalaya), R-II (Kakul–Cherat Hills, Swat Valley, Margalla Hills, Azad Jammu and Kashmir, Jhelum River Basin, Southwestern Himalaya), and R-III (Central KPK, southern parts of Kabul River Basin).

Table 1. A detailed description of the selected meteorological stations in northern Pakistan.

No.	Code	Stations	Region	Duration	Elevation (m)	Latitude	Longitude	Coefficient of Variance
1	Nlt	Naltar	I	1995–2012	2858	36.17	74.18	0.19
2	Zrt	Ziarat		1995–2012	3669	36.49	74.26	0.51
3	Khu	Khunjerab		1995–2012	4730	36.84	75.42	0.31
4	Ast	Astor		1960–2016	2168	35.35	74.86	0.25
5	Bun	Bunji		1960–2016	1372	35.67	74.63	0.44
6	Chl	Chilas		1960–2016	1250	35.42	74.1	0.48
7	Glt	Gilgit		1960–2016	1460	35.92	74.33	0.35
8	Gup	Gupis		1960–2016	2156	36.17	73.4	0.73
9	Skd	Skardu		1960–2016	2317	35.18	75.68	0.51
10	Cht	Chitral		1964–2016	1498	35.83	71.78	0.28
11	Drh	Drosh		1960–2016	1465	35.55	71.85	0.24
12	Dir	Dir	II	1967–2016	1375	35.2	71.85	0.19
13	Sad	Saidu Sharif		1974–2016	961	34.73	72.35	0.22
14	Gdp	Garhi Dupatta		1960–2016	813	34.13	73.47	0.19
15	Ktl	Kotli		1960–2016	614	33.31	73.54	0.21
16	Mzf	Muzaffarabad		1960–2016	838	34.37	73.48	0.17
17	Blk	Balakot		1960–2016	995	34.55	73.21	0.22
18	Mur	Murree		1960–2016	2134	33.90	73.40	0.17
19	Kak	Kakul		1960–2016	1775	34.18	73.15	0.14
20	Cht	Cherat		1960–2016	1372	33.92	71.9	0.34
21	Isb	Islamabad		1960–2016	508	33.80	73.08	0.25
22	Pch	Parachinar	III	1960–2016	1775	33.90	70.10	0.42
23	Psh	Peshawar		1960–2016	328	34.02	71.58	0.34
24	Rsp	Risalpur		1960–2016	304	34.07	71.98	0.29
25	Kht	Kohat		1960–2016	564	33.45	71.53	0.31

Table 2. Distribution of major regions and number of metrological stations in different climate zones of Pakistan.

Region	Characteristics	Major Regions	Stations
I	Semi-arid	Gilgit–Baltistan and Chitral region, Upper Indus Basin and Chitral River Basin, Hindukush–Karakoram–Himalaya	11
II	Humid	Kakul–Cherat Hills, Swat Valley, Margalla Hills, Azad Jammu and Kashmir, Jhelum River Basin, Southwestern Himalaya	10
III	Humid	Central KPK, southern parts of Kabul River Basin	4

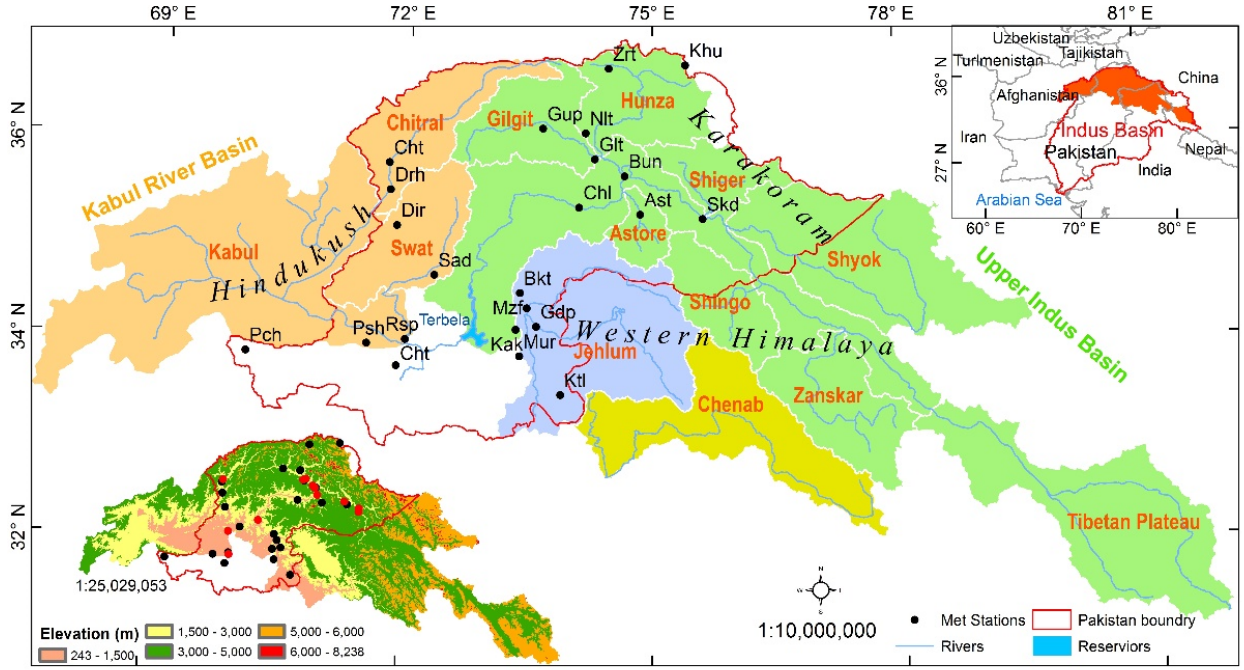

Figure 1. Spatial distribution of meteorological stations in different sub-basins in northern Pakistan. The red outline indicates the boundary of the Upper Indus basin with the administration of northern Pakistan.

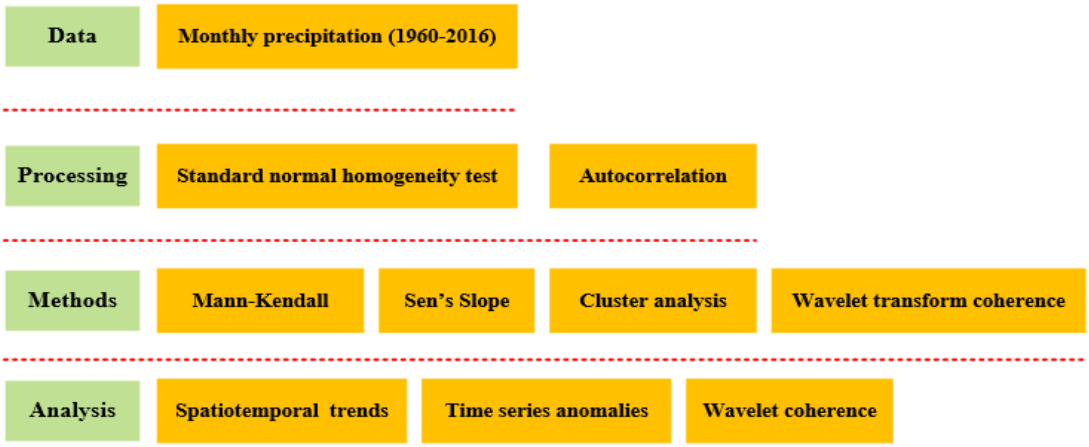

Figure 2. Flow chart of the data pre-processing, methodology, and analysis used.

3.2. Mann—Kendall Test and Sen's Slop Estimator

The non-parametric Mann–Kendall (MK) test is a commonly used test to identify trends in various time series because it is unaffected by the normal distribution of data time series and outliers [30,47–51]. Two hypotheses (null and alternative) are used in this test identify the trend direction. The null hypothesis shows no trend in the time series, while the alternative indicates an increasing or decreasing trend. The determined Z value of this test follows the normal distribution with a variance average (0, 1) used to detect trend significance. So, according to this, an increasing trend is shown by $Z > 0$, and vice versa [52–54]. In addition, Sen's slope estimator (SSE) determined the magnitude of the precipitation time series trend by a simple non-parametric procedure [43,55,56].

3.3. The Sequential Mann–Kendall Test (SQMK) Test

Sneyers introduced the SQMK test to analyze the significant change points in long-term time series [57–62]. The abrupt change in the trend is analyzed by the forward (SF)

and backward (SB) sequential series. SF has sequential behavior, which changes around zero because SF is a standardized variable with a zero mean and unit standard deviation. In addition, it has the exact nature of Z values that start from the first point of the time series to the last point of the time series. On the other hand, SB is opposite to Z values as it moves from the last point to the start point of the time series [63,64]. In this study, we chose a 5% significance level. A negative trend is shown when both SF and SB have decreasing values; on the other hand, a positive trend is shown when SF and SB have increasing values [65]. SF and SB intersect at a specific point describing a major abrupt change in that year in the time series [20].

3.4. Cluster Analysis

The use of clustering algorithms provides for the efficient division of big data sets into homogeneous clusters by acquiring knowledge [66,67]. The k-means cluster algorithm approach described by [67] carries out the following fundamental steps: (a) the procedure first establishes the centers of the K number of clusters, and then each variable is assigned to the closest cluster center using only a similarity metric. (b) After assigning each parameter to a cluster as input data, all groups are recalculated for cluster centers. (c) The factors may be distributed among different clusters depending on where the new cluster centers are located. The "distance measure" is used to determine the correlations of variables to cluster centers, and this strategy is continued until there is no modification in the cluster centers [68].

3.5. WTC Analysis

Wavelet coherence analysis (WTC) is a statistical tool used in signal processing and time-series analysis to examine the relationship between two signals as a function of time and frequency [69]. WTC involves using wavelet transforms, mathematical tools that can decompose signals into their frequency components and provide information on the power and phase of each frequency component. It transforms the two signals and then calculates their coherence at each frequency and time point [70]. The coherence value ranges from 0 to 1, where zero indicates no relationship between the two signals, and one indicates a perfect linear relationship between the two signals. WTC has applications in various fields, including neuroscience, environmental science, and economics [71]. Recently, Hussain et al. [69] analyzed the cross-correlation between precipitation series and large-scale climate indices using the WTC. The extent of a linear association in the time and frequency domain is assessed using this correlation coefficient, which is localized in the time and frequency domain [72]. The Monte Carlo approach calculates the significance level in WTC, and the cone of influence is used to calculate the significance level [73]. WTC displays the 95% confidence levels corresponding to the pink noise and draws attention to the significant coherence even though the common power of both variables is low.

4. Results

4.1. Climatology

The spatial distribution of the mean seasonal and annual precipitation in the different regions of NP is shown in Figure 3, while the sub-regional amounts are presented in Table 3. The results depict that the stations located in R-II received the highest mean precipitation annually, while stations in R-I received less precipitation annually. The stations located in R-III received high annual precipitation, but the precipitation amount was limited in autumn. NP's observed mean annual precipitation was 823 mm (Table 3). Annual and summer mean precipitation in R-II was 1320 mm and 556 mm, respectively. However, winter, spring, and autumn had below 350 mm of precipitation. Among all regions, R-II received the highest precipitation at seasonal and annual scales, followed by R-III and R-I (Table 3 and Figure 3). The amount of seasonal and annual precipitation was below 250 and 700 mm in R-I and III, respectively. Overall, maximum precipitation was obvious in summer, followed by spring and winter (Table 3).

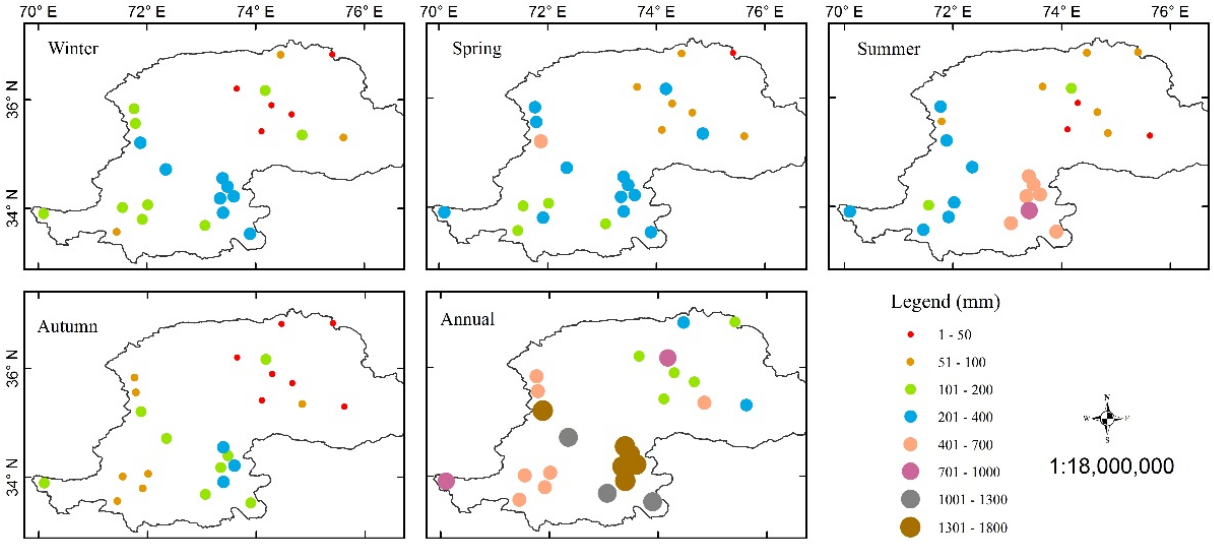

Figure 3. Spatial distribution of mean seasonal and annual precipitation (mm/decade) in northern Pakistan.

Table 3. Mean seasonal and annual precipitation in different sub-regions of northern Pakistan.

	Winter	Spring	Summer	Autumn	Annual
R-I	48.42	103.75	47.68	28.80	229.54
R-II	259.59	324.80	556.88	178.25	1320.57
R-III	128.05	212.37	232.67	89.99	664.81
NP	166.48	237.06	308.63	110.52	823.80

4.2. Spatiotemporal Trends

The spatial distribution of MK and SSE trends for seasonal and annual precipitation in NP are shown in Figure 4, whereas regional trends during 1960–2016 are presented in Table 4. It is worth mentioning that the station density in the NP was very sparsely distributed, and the number of stations with long-term observed datasets was very limited. Therefore, we also used ERA-5 reanalysis precipitation data to supplement the observed dataset in reproducing the spatial distribution of precipitation in the whole region. The spatial trend of ERA-5 reanalysis datasets in NP is presented in Figure 5.

Table 4. Mann–Kendall and Sen's slope trends for seasonal and annual precipitation (mm/decade) in different sub-regions of northern Pakistan. Bold indicates 5% significance levels.

Period		Winter	Spring	Summer	Autumn	Annual
1960–1988	R-I	−0.11	−0.52	**0.88**	0.37	1.53
	R-II	−0.13	1.35	1.19	0.43	5.94
	R-III	−0.98	−1.69	0.84	**−1.02**	−3.35
	NP	−0.18	0.38	2.07	0.24	3.33
1989–2016	R-I	−0.28	−0.87	−0.58	0.20	−0.45
	R-II	−5.24	−3.14	−2.92	−0.21	−7.90
	R-III	0.08	2.80	**5.49**	2.24	**12.55**
	NP	−2.76	−1.19	−0.54	0.43	−1.91
1960–2016	R-I	0.38	−0.15	**0.39**	0.12	**1.05**
	R-II	−0.34	−0.40	−1	0.00	−1.14
	R-III	0.57	0.20	**1.64**	0.63	**3.95**
	NP	−0.55	−0.75	−1.66	−0.19	−2.86

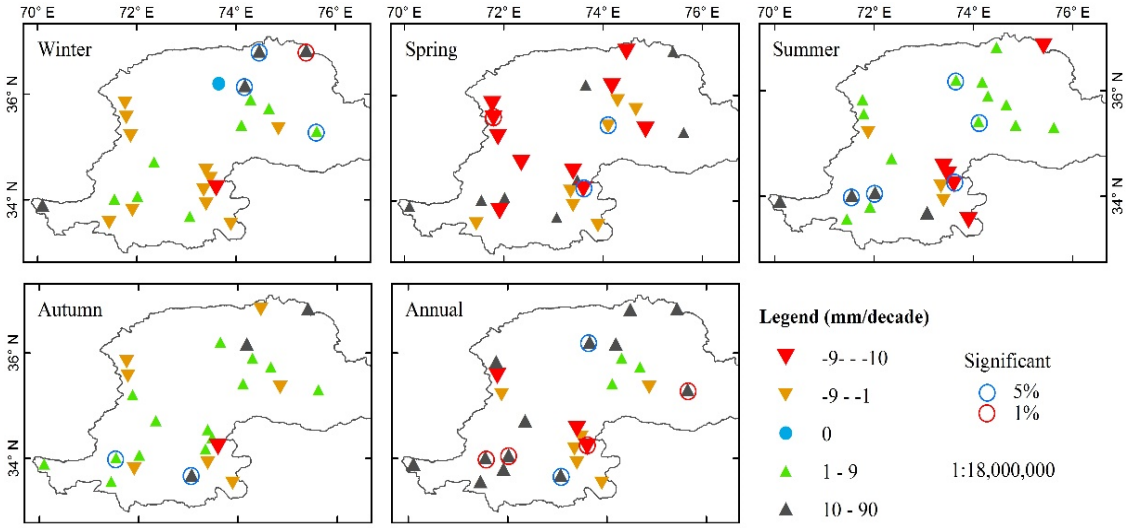

Figure 4. Spatial distribution of Mann–Kendall and Sen's seasonal and annual precipitation trends in northern Pakistan.

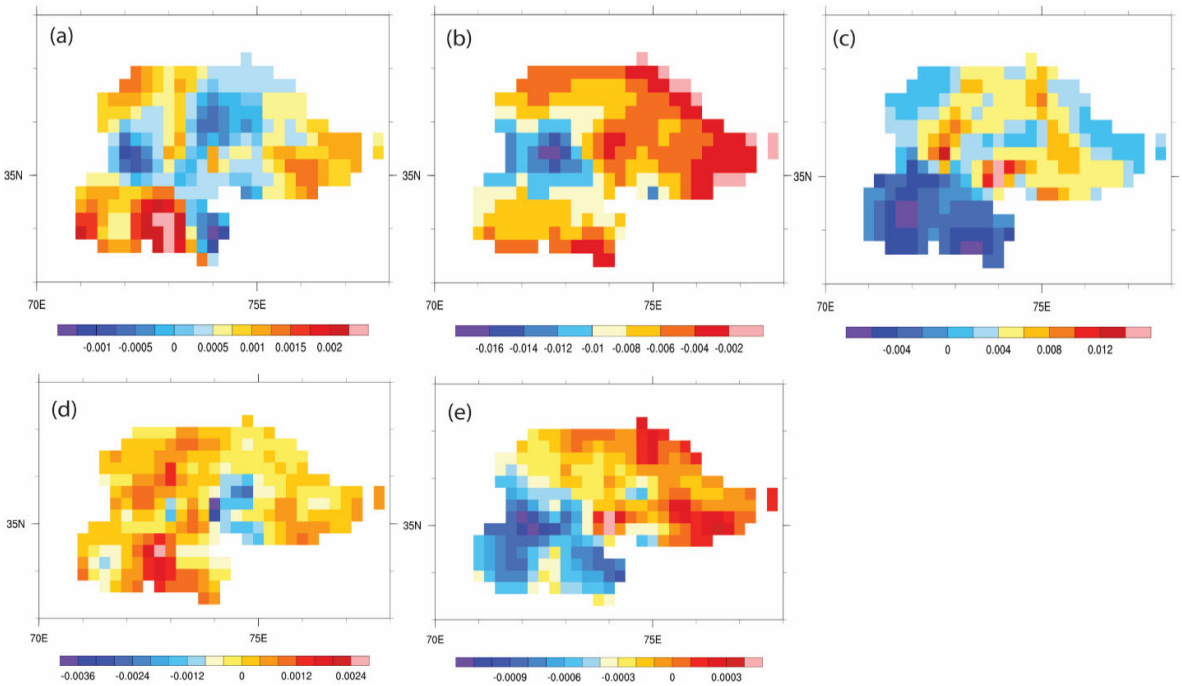

Figure 5. Spatial distribution of (**a**) winter, (**b**) spring, (**c**) summer, (**d**) autumn, and (**e**) annual precipitation trends with ERA-5 reanalysis datasets in northern Pakistan.

Winter precipitation showed an increasing (decreasing) trend at 13 (12) stations (Figure 4), whereas ERA-5 also displayed similar results; the southern and eastern region in NP Pakistan showed increasing trends, while decreasing in the remaining sites (Figure 5). The lowest negative slopes were observed in stations of R-II; however, Naltar, Khunjerab, and Ziarat observed significant increasing trends. Most of the stations in R-II displayed negative trends (Figure 4). Winter precipitation in NP shows mixed trends, whereas increasing trends were observed in the R-I and III at a rate of 0.38 and 0.57 mm/decade, respectively. During the study period (1960–2016), R-II and NP kept decreasing trends at −0.34 and −0.55 mm/decade, respectively (Table 4). In the spring, the negative trend was evident over the whole NP with a significant decreasing trend in Astor (Figure 4). Spring precipitation decreased in R-I, II, and NP at the rates of −0.15, −0.40,

and −0.75 mm/decade, respectively, while only an increase was observed in R-III during the study period (Table 4). The observed results agreed with the ERA-5 reanalysis trends (Figure 5), as the region indicated a decreasing trend. In summer, the positive trends were obvious over R-I and R-III, while most stations in R-II exhibited negative trends (Figure 4), whereas summer precipitation decreased in R-II and III, while an increasing trend was obvious in R-I as observed in ERA-5 datasets (Figure 5). R-I and III exhibited significant positive trends at the rates of 0.39 and 1.64 mm/decade, respectively, whereas R-II and NP observed negative trends (Table 4). A mixture of positive and negative trends from 1960 to 2016 was evident in autumn.

Autumn showed an increasing (decreasing) trend at 16 (08) stations (Figure 4), whereas increasing trends were more dominant, as observed in ERA-5 datasets in the whole region (Figure 5). Such increasing trends were more dominant in R-II, II, and in western parts of R-I. In R-I, most stations showed positive trends; in R-III, all stations exhibited positive trends. According to the MK outcomes, Darosh and Murree witnessed significant negative trends, while Peshawar, Risalpur, Kakul, Skardu, and Gupis showed significant positive trends (Figure 4). All three sub-regions had positive trends in autumn from 1960 to 2016 (Table 4). Most stations in R-I and III observed increasing trends, while they decreased in R-II for annual precipitation (Figure 4). However, increasing trends were more prominent in R-I, whereas decreasing trends were obvious in R-II and III, as observed in the ERA-5 reanalysis results. Moreover, R-I and III observed significant increasing trends in annual precipitation at a rate of 1.05 and 3.95 mm/decade, respectively, and decreasing trends in R-II and NP during 1960–2016 (Table 4). Overall, the trends for observed data and ERA-5 reanalysis datasets were almost similar in winter, spring, and autumn; however, some disagreement was observed in both datasets in summer and annual precipitation trends in NP. The region is known for its complex topography, which can lead to significant orographic effects on precipitation patterns, particularly during the summer monsoon, whereas variations in atmospheric circulation patterns, such as the strength and position of the westerly jet stream, may also influence precipitation patterns in the region [74]. The disagreement between observed data and ERA-5 reanalysis datasets in the NP could be due to the complex topography of the region, which can lead to significant orographic effects on precipitation patterns [75]. Additionally, the influence of the South Asian Summer Monsoon and variations in vegetation cover and atmospheric circulation patterns may also contribute to discrepancies between the datasets and due to the combination of factors in NP [76].

For a more detailed and systematic analysis, the whole period was divided into two sub-periods, i.e., 1960–1988 and 1989–2016 (Table 4). In winter, precipitation in R-I, II, II, and NP decreased during 1960–1988, which was also prominent in the second period, except for an increase in R-III with 0.08 mm/decade. For spring, precipitation increased during 1960–1988 in NP but decreased during 1989–2016; however, mixed trends prevailed in the sub-regions in both periods. Summer precipitation increased in the first period in all sub-regions and NP, while a decrease was observed in R-I, II, and NP. Autumn showed steadily increasing trends in both periods in all sub-regions. Furthermore, annual precipitation in NP increased in the first period at a rate of 3.33 mm/decade, decreasing in the second period at a rate of −1.91 mm/decade, respectively.

4.3. Temporal Variations

Anomalies for annual and seasonal precipitation are shown in Figure 6. No clear trends were observed in NP for winter precipitation until the mid-1980s, but an increasing trend was apparent afterward. The increasing trend was also prominent annually, with the anomalies dominated by positive values from the mid-1980s onwards. The anomaly values kept changing for spring, summer, and autumn without any clear trend.

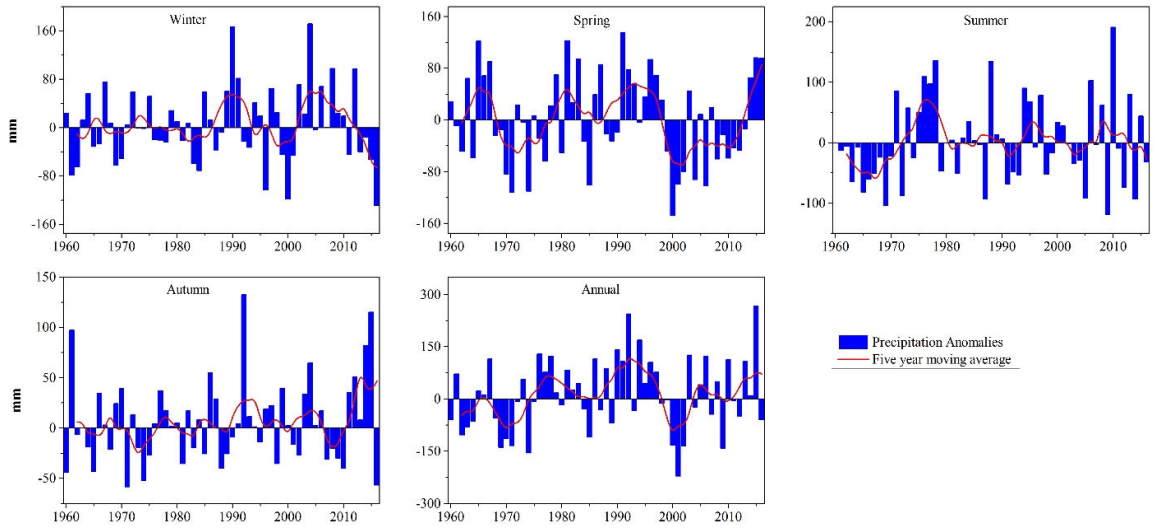

Figure 6. Seasonal and annual time-series anomalies relative to 1961–1990 mean values for seasonal and annual precipitation in northern Pakistan. The smooth line indicates a five-year moving average.

The SQMK analysis was further employed to assess the abrupt shifts in seasonal and annual precipitation in NP, and the results are shown in Figure 7. In winter, abrupt shifts were observed between 1961 and 1985, while a rapid upward shift was evident after the mid-1980s until 2010. Significant abrupt changes in spring were detected during 1967–1980. A sharp decreasing shift was observed in 1967. An increasing trend was observed in 1980, while a downward trend was evident from mid-2000 onwards. In summer, there was a clear increasing trend until 1975; however, a decreasing trend was noticeable afterward. Similarly, autumn showed an increasing trend until 2010. Annual precipitation showed an increasing trend from the mid-1970s onwards; however, a major downward trend was obvious after 2000.

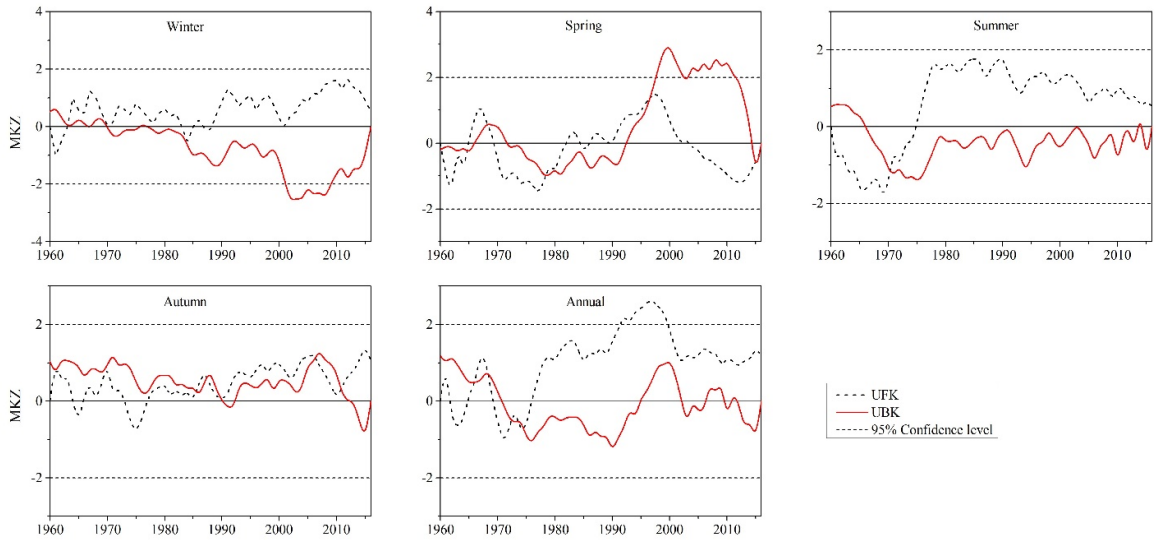

Figure 7. Temporal changes of Z value based on the Mann–Kendall test for seasonal and annual precipitation in northern Pakistan.

The temporal trends in annual precipitation were assessed over six different elevation zones in NP (Figure 8). The various elevation zones were <500 m, 500–1000 m, 1000–1500 m, 1500–2000 m, 2000–2500 m, and 2500–5000 m. The annual precipitation showed an increasing trend in <500 m, 100–1500 m, 1500–2000 m, 2000–2500 m, and 2500–5000 m, whereas a decreasing trend was observed in 500–1000 m.

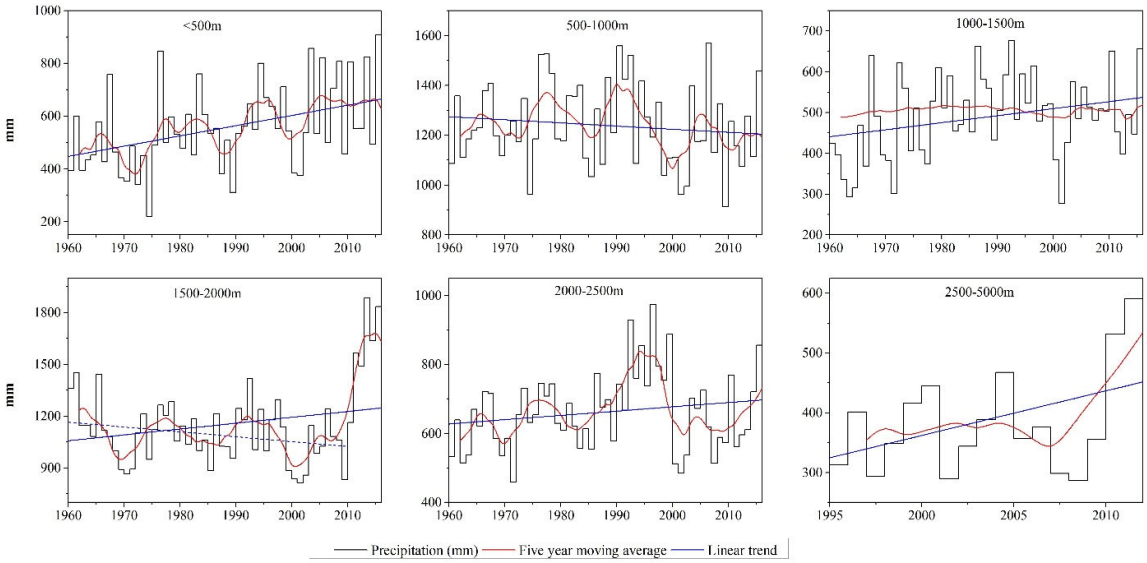

Figure 8. Temporal trends of annual precipitation in northern Pakistan. The blue line indicates linear trends, while the red line is the five-year moving mean.

4.4. Coherence of Precipitation with Teleconnections

Figure 9 displays the WTC results for the AMO, AO, NAO, ENSO, IOD, and PDO over NP from 1960 to 2016. The pink color shows the percent area of significant coherence (PASC) relative to the total area, and black circles with pink colors show high coherence. In this study, the WTC analysis was preferred over other methods because it indicates the coherences over time and space [65]. However, traditional correlation or regression analysis can only give one value with the degree of linear correlation between two variables. The WTC indicated the temporal signals of various teleconnections with the regional precipitation at interannual, decadal, and interdecadal scales. Significant interdecadal coherences were evident with the AO and PDO from 128 months and above, whereas most significant interannual coherences in the ENSO were found at 16–128 months (Figure 9). Moreover, the AO, ENSO, and IOD witnessed higher coherence with precipitation in NP, whereas the AMO, NAO, and PDO observed fewer coherences. The observed findings of the AO, IOD, PDO, and ENSO agreed with the results reported by [69] in the monsoon region of Pakistan.

Changes in precipitation on a monthly time scale differ from those on seasonal and yearly scales, as different indices have different degrees of effect throughout multiple seasons. For instance, the dominating factors that impact many regions of the planet are the large-scale modes in the AO, NAO, ENSO, and PDO, each operating at a very different time. Therefore, we further explored the precipitation association on seasonal and annual scales using regression analysis to complement the wavelet coherence. Table 5 shows the regression of oceanic indices with regionally averaged seasonal and annual precipitation. The regression values of 3.40 and 1.97 suggested a linear association of winter precipitation with the AO and ENSO, respectively, and a negative association of precipitation with the NAO, IOD, and PDO indices at the rates of −2.28, −2.40, and −1.08, respectively. The regression coefficients of 1.86 and 0.08 showed linear spring precipitation association with the ENSO and PDO, respectively. On the other hand, a negative association of precipitation with the AO, NAO, and IOD was evident, having −0.21, −0.32, and −4.40 regression, respectively. The regression values of 1.27, 0.68, and 1.11 suggested a linear association of summer precipitation with the AO, IOD, and PDO, respectively, and a negative association between the NAO and ENSO at −1.12 and −1.33, respectively. On the annual scale, a positive relationship with the AO, ENSO, and PDO at 3.34, 2.19, and 0.63, respectively, was found, while a negative relationship with NAO (−1.28) and IOD (−6.10) was observed. Overall, winter precipitation had a higher linear regression with the AO and spring with

ENSO, while the AO, IOD, and PDO had more influence during summer, and the AO and ENSO were dominant at annual time scales.

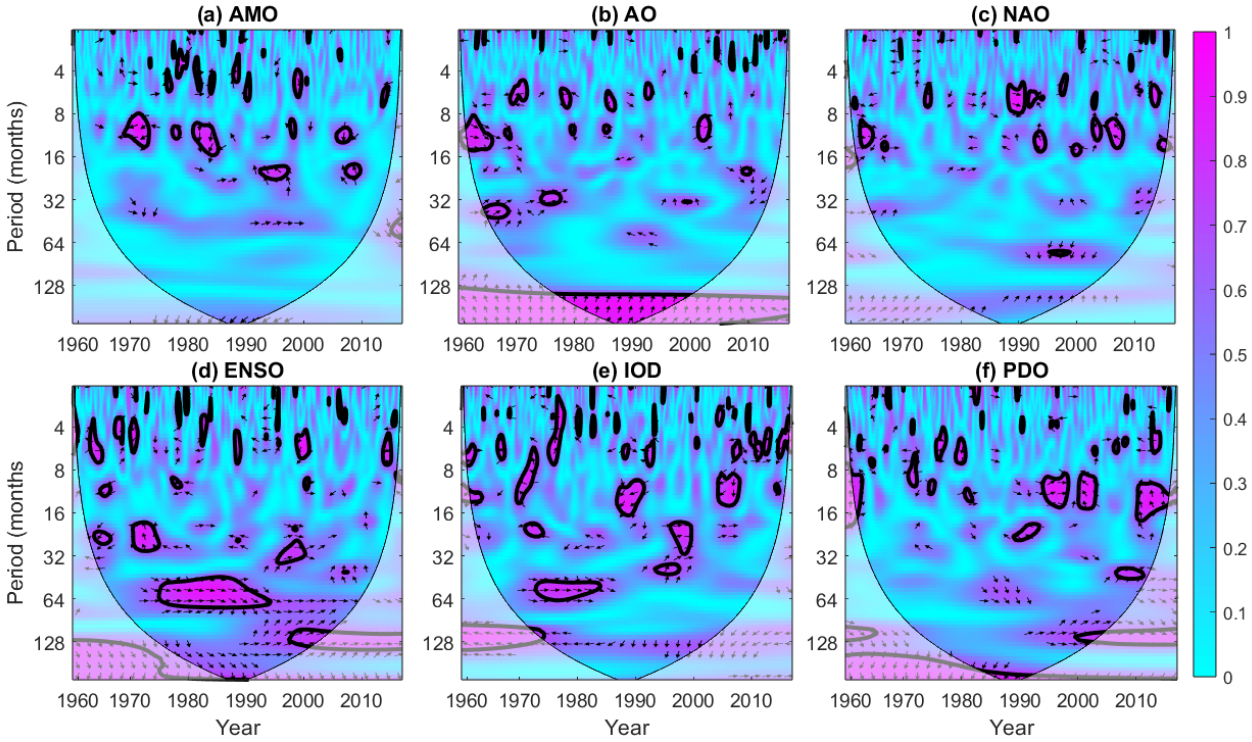

Figure 9. Wavelet coherence between monthly precipitation over northern Pakistan with (**a**) the AMO, (**b**) AO, (**c**) NAO, (**d**) ENSO, (**e**) IOD, and (**f**) PDO. Right-pointing arrows indicate that the two signals are in phase, while the left is for antiphase signals. Thick contours denote 5% significance levels against pink noise.

Table 5. Regression of oceanic indices with regionally averaged seasonal and annual precipitation.

Season	Index	Estimate	SE	*p*-Value
Winter	AO	3.40	1.08	0.002
	NAO	−2.28	0.77	0.004
	ENSO	1.97	0.72	0.008
	IOD	−2.40	1.71	0.16
	PDO	−1.08	0.45	0.02
Spring	AO	−0.21	1.22	0.85
	NAO	−0.32	0.87	0.71
	ENSO	1.86	0.81	0.02
	IOD	−4.40	1.92	0.02
	PDO	0.08	0.52	0.87
Summer	AO	1.27	0.78	0.10
	NAO	−1.12	0.56	0.04
	ENSO	−1.33	0.52	0.01
	IOD	0.68	1.23	0.58
	PDO	1.11	0.33	0.001
Annual	AO	3.34	1.54	0.03
	NAO	−1.28	1.10	0.24
	ENSO	2.19	1.02	0.037
	IOD	−6.10	2.43	0.01
	PDO	0.63	0.65	0.33

5. Discussion

Due to the frequent and intense climatic events, sensitive places are anticipated to be exposed exponentially over the globe to floods and droughts, which can raise associated risk and susceptibility [77]. For most of Pakistan, the northern sub-Himalayan region is the country's primary water source and is highly sensitive to climate change. Pakistan's hydrology and water security may be severely affected by changes in precipitation in NP. The non-parametric MK, SSE, SQMK, and WTC analyses were used to observe the trends and precipitation relations with oceanic indices.

Results inferred maximum precipitation for annual and summer timeframes (Figure 3, Table 3), which agrees with numerous studies [23,78]. The spatial and temporal trends for seasonal and annual precipitation over different sub-climatic regions showed that the trend's magnitude varied from region to region and station to station [51]. Annual and summer mean precipitation in R-II was 1320 and 556 mm, respectively. Results showed that annual and summer mean precipitation was highest, especially in R-II [51,79]. The seasonal and annual precipitation trends decreased in NP during 1960–2016, while summer and annual precipitation significantly increased in R-I and R-III [30]. R-II and III were influenced by monsoons and westerlies [20].

In two sub-periods, 1960–1988 and 1989–2016, precipitation in R-I, II, III, and NP declined in the winter from 1960 to 1988. This trend was still apparent in the second period [30], except for an increase in R-III. Precipitation in spring increased in NP in both periods; nevertheless, mixed trends dominated the sub-regions [80]. All sub-regions and NP experienced increased summer precipitation [69] during the first period. Additionally, the annual precipitation in NP changed with time [24], increasing in the first sub-period and decreasing in the second sub-period of the study period (Table 4). These results are consistent with the findings of [24,81,82]. It was explained earlier that there has been a noticeable increase in the amount of precipitation during the South Asian summer monsoon, sometimes with wet extremes, which is mostly due to the East Asian summer monsoon's penetration and a western disturbance over the country's northern mountainous regions [83]. There are indicators that strong and widespread human activity in Asia has begun to disrupt the monsoon season [30,84], while La Nina's influence supports high summer monsoon rainfall over South Asia [85]. Furthermore, the monsoon may be shifting west, carrying more moisture and producing additional rains and extreme events across Pakistan [81]. Summer and annual precipitation in R-III significantly increased during 1960–2016. These findings are consistent with the results of [86], whereas [87,88] explained and attributed it to the projected increase in the South Asian summer monsoon precipitation status under enhanced greenhouse gas emission scenarios.

The anomaly values fluctuated throughout spring, summer, and autumn with no discernible pattern [89]. The rising precipitation shows that the region's monsoons are getting stronger. The monsoons are becoming less frequent but more potent in some parts of South Asia, increasing the likelihood of catastrophic weather events there [20]. Until the middle of the 1980s, there were often no discernible patterns in the amount of winter precipitation in NP [76], but from 1985 to 2005, there was a distinct upward trend. Such growing tendencies are also present in annual data, with positive values dominating the anomalies from the middle of the 1980s to 2016. Similar results are consistent with [81,82,90].

Wintertime significant shifts were seen between 1961 and 1985 [91], and from the mid-1980s to 2010 there has been a rapidly increasing shift. Between 1967 and 1980, spring underwent its most significant dramatic changes. In 1967, a sudden diminishing shift was noticed (Figure 6). While there was an upward tendency in 1980, there has been a downward trend since about mid-2000. Until 1975, there was a noticeable upward trend for the summer but a definite downward trend [92]. The same is true for the autumn precipitation trend in 2010. From the middle of the 1970s onward, annual precipitation indicated an increasing trend [82]; however, after 2000, a significant declining trend was evident. These results are in good agreement with those of [29,51].

Throughout the study period, various trends were visible in the annual precipitation at various altitudes. Past studies showed a positive correlation between precipitation and elevation [93,94]. The annual precipitation increased in the altitude zones of 500 m, 100–1500 m, 1500–2000 m, 2000–2500 m, and 250–5000 m. The deepening of the land–sea thermal contrast, which enhances moisture flux transfer from the ocean toward the land, may have caused an increasing precipitation trend. In contrast, a declining tendency was seen in the 500–1000 m elevation range. Between 1960 and 2016, significant interdecadal coherences with the AO and PDO spanning from 128 months and above were noticed. The ENSO's most notable interannual coherences were during 16–128 months. In contrast to the AMO, NAO, and PDO, the AO, ENSO, and IOD generally showed higher coherences with precipitation in NP [20,69].

Studies found a considerable rise in maximum and minimum temperatures over Pakistan between 1980 and 2016, which may have significantly affected precipitation [16]. According to Hussain and Lee [95], widespread urbanization and a sharp rise in population in the middle and upper Punjab, particularly after the 1980s, are two potential causes of rising precipitation. Such variations may be brought on by mechanical variability induced by increased surface lumpiness and sensible heat from the warm metropolitan air. Additionally, an increase in precipitation in South Asia is due to the vapor transfer from the Arabian Sea and the Bay of Bengal [96,97]. A recent trend towards a lesser monsoonal effect was shown by a change in long-term summer wetting to drying between 1995–2012 [98]. A decrease in the north–south sea surface temperature gradient across the North Indian Ocean and the monsoon circulation over Pakistan is to blame for the dip in rainfall activity [99].

Moreover, de Oliveira-Júnior et al. [100] discovered that the ENSO greatly impacts Pakistan's yearly precipitation. They also studied how the AMO and PDO affected precipitation variability in the UIB. Attada et al. [101] revealed strong associations between the mean temperature and the global teleconnections with the NAO and ENSO during the spring, which is how the NAO might affect certain monsoon months, particularly August. In the southern regions of Central Asia, winter precipitation is significantly influenced by the NAO and ENSO. The Indian monsoon, which controls the southern portion of Central Asia, can be severely impacted by the warm phase of the AMO concurrently [102]. According to another study, the NAO and ENSO precipitation signals in Central Southwest Asia are mostly related to an intensification of westerlies that move eastward across the territory of Central Southwest Asia (including northern Pakistan) during the positive NAO and the warm ENSO phases [103].

6. Conclusions

The present study used non-parametric MK, SSE, SQMK, cluster analysis, and WTC analyses to observe seasonal and annual precipitation trends, variability, and teleconnections. Based on the current study's findings and detailed literature, there is a need to assess the influencing mechanism systematically and comprehensively.

1. In the spatial distribution of mean seasonal and annual precipitation, all regions received the highest precipitation annually. R-II received the highest precipitation at seasonal and annual scales, followed by R-III and I. At the same time, R-I and III received seasonal and annual precipitation below 250 and 700 mm, respectively. Generally, maximum precipitation is observed in summer, followed by spring and winter. According to the MK and SS, most stations in R-I and III observed increasing trends, while decreased in R-II were observed for annual precipitation. Moreover, R-I and III observed significant increasing trends in annual precipitation and decreasing trends in R-II and NP during 1960–2016. Moreover, the spatial trends for observed data and ERA-5 reanalysis datasets were almost similar in winter, spring, and autumn; however, some disagreements were observed in both datasets in summer and annual precipitation trends in NP.
2. The whole period was divided into two sub-periods, which were 1960–1988 and 1989–2016. In winter, precipitation in R-I, II, III, and NP decreased during 1960–1988,

which was also prominent in the second period. For spring, precipitation increased during the first period in NP while decreasing during the second time scale; however, mixed trends prevailed in both time scales. Summer precipitation increased in the first period in all sub-regions and NP, while a decrease was observed in R-I, II, and NP. Autumn showed steadily increasing trends in both periods in all sub-regions. Furthermore, annual precipitation in NP increased in the first period and decreased in the second.

3. In temporal variations, no clear trend was observed in all seasons except in annual and winter periods. An increasing trend was evident in annual and winter periods during 1985–2016 and 1985–2005, respectively. According to the SQMK, most trends increased in all seasons until 1980, and a downward shift occurred after 2010.
4. The temporal trends in annual precipitation were assessed over six elevations. The annual precipitation showed an increasing trend at <500 m, 100–1500 m, 1500–2000 m, 2000–2500 m, and 2500–5000 m, whereas the decreasing trend is observed at 500–1000 m. According to WTC, the AO, ENSO, and IOD witnessed higher coherence with precipitation in NP, whereas the AMO, NAO, and PDO observed fewer coherences.
5. Winter precipitation had a higher linear regression with AO and spring with ENSO, while the AO, IOD, and PDO have higher influences on summer precipitation, whereas the AO and ENSO were dominant at the annual time scale.

Author Contributions: Conceptualization: A.H.; Methodology: A.H. and I.H.; Formal analysis and investigation: A.R. and A.H.; Writing—original draft preparation: A.R. and A.H.; Writing—review and editing A.R., A.H., W.U., H.A. and S.U., Funding: J.Z. and J.C. All authors have read and agreed to the published version of the manuscript.

Funding: The National Natural Science Foundation of China, Grant No. 31870707.

Institutional Review Board Statement: Not applicable.

Informed Consent Statement: Not applicable.

Data Availability Statement: The observed dataset can officially acquire from Pakistan Meteorology Department.

Acknowledgments: The authors acknowledge the Pakistan Meteorology Department for providing precipitation data for this research. The ERA5-Reanalysis data can be downloaded from the website: https://cds.climate.copernicus.eu/cdsapp#!/search?type=dataset, and is officially accessed on 28 April 2023.

Conflicts of Interest: The authors declare no conflict of interest.

References

1. Perotti, E.; Huguenin-Elie, O.; Meisser, M.; Dubois, S.; Probo, M.; Mariotte, P. Climatic, soil, and vegetation drivers of forage yield and quality differ across the first three growth cycles of intensively managed permanent grasslands. *Eur. J. Agron.* **2021**, *122*, 126194. [CrossRef]
2. Palmer, M.; Ruhi, A. Linkages between flow regime, biota, and ecosystem processes: Implications for river restoration. *Science* **2019**, *365*, eaaw2087. [CrossRef] [PubMed]
3. Li, X.; Zhang, K.; Gu, P.; Feng, H.; Yin, Y.; Chen, W.; Cheng, B. Changes in precipitation extremes in the Yangtze River Basin during 1960–2019 and the association with global warming, ENSO, and local effects. *Sci. Total Environ.* **2021**, *760*, 144244. [CrossRef]
4. Hrudya, P.; Varikoden, H.; Vishnu, R. A review on the Indian summer monsoon rainfall, variability and its association with ENSO and IOD. *Meteor. Atmos. Phy.* **2021**, *133*, 1–14. [CrossRef]
5. Papalexiou, S.M.; Montanari, A. Global and regional increase of precipitation extremes under global warming. *Water Resour. Res.* **2019**, *55*, 4901–4914. [CrossRef]
6. Reichle, R.H.; Koster, R.D.; De Lannoy, G.J.; Forman, B.A.; Liu, Q.; Mahanama, S.P.; Touré, A. Assessment and enhancement of MERRA land surface hydrology estimates. *J. Clim.* **2011**, *24*, 6322–6338. [CrossRef]
7. Zhang, Y.; You, Q.; Ullah, S.; Chen, C.; Shen, L.; Liu, Z. Substantial increase in abrupt shifts between drought and flood events in China based on observations and model simulations. *Sci. Total Environ.* **2023**, *876*, 162822. [CrossRef]
8. Yu, Y.; You, Q.; Zuo, Z.; Zhang, Y.; Cai, Z.; Li, W.; Jiang, Z.; Ullah, S.; Tang, X.; Zhang, R. Compound climate extremes in China: Trends, causes, and projections. *Atmos. Res.* **2023**, *286*, 106675. [CrossRef]

9. Tuel, A.; Martius, O. A global perspective on the sub-seasonal clustering of precipitation extremes. *Weather. Clim. Extrem.* **2021**, *33*, 100348. [CrossRef]
10. Rivera-ferre, M.; Di Masso, M.; Vara, I.; Cuellar, M.; López-i-Gelats, F.; Bhatta, G.; Gallar, D. Traditional agricultural knowledge in land management: The potential contributions of ethnographic research to climate change adaptation in India, Bangladesh, Nepal, and Pakistan. *Clim. Develop.* **2021**, *13*, 644–661. [CrossRef]
11. Waqas, H.; Lu, L.; Tariq, A.; Li, Q.; Baqa, M.F.; Xing, J.; Sajjad, A. Flash Flood Susceptibility Assessment and Zonation Using an Integrating Analytic Hierarchy Process and Frequency Ratio Model for the Chitral District, Khyber Pakhtunkhwa, Pakistan. *Water* **2021**, *13*, 1650. [CrossRef]
12. Eckstein, D.; Künzel, V.; Schäfer, L. Global Climate Risk Index 2021, Who Suffers Most from Extreme Weather Events. In *Weather-Related Loss Events in 2019 and 2000–2019*; Germanwatch eV: Bonn, Germany, 2021.
13. Abbas, A.; Bhatti, A.S.; Ullah, S.; Ullah, W.; Waseem, M.; Zhao, C.; Dou, X.; Ali, G. Projection of precipitation extremes over South Asia from CMIP6 GCMs. *J. Arid Land* **2023**, *15*, 274–296. [CrossRef]
14. Hu, P.; Sharifi, A.; Tahir, M.N.; Tariq, A.; Zhang, L.; Mumtaz, F.; Shah, S.H.I.A. Evaluation of Vegetation Indices and Phenological Metrics Using Time-Series MODIS Data for Monitoring Vegetation Change in Punjab, Pakistan. *Water* **2021**, *13*, 2550. [CrossRef]
15. Arshad, M.; Ma, X.; Yin, J.; Ullah, W.; Ali, G.; Ullah, S.; Liu, M.; Shahzaman, M.; Ullah, I. Evaluation of GPM-IMERG and TRMM-3B42 precipitation products over Pakistan. *Atmos. Res.* **2021**, *249*, 105341. [CrossRef]
16. Ullah, W.; Wang, G.; Ali, G.; Tawia Hagan, D.F.; Bhatti, A.S.; Lou, D. Comparing multiple precipitation products against in-situ observations over different climate regions of Pakistan. *Remote Sens.* **2019**, *11*, 628. [CrossRef]
17. Lau, W.K.; Kim, K.-M. The 2010 Pakistan flood and Russian heat wave: Teleconnection of hydrometeorological extremes. *J. Hydromet.* **2012**, *13*, 392–403. [CrossRef]
18. Wu, H.; Guo, B.; Fan, J.; Yang, F.; Han, B.; Wei, C.; Lu, Y.; Zang, W.; Zhen, X.; Meng, C. A novel remote sensing ecological vulnerability index on large scale: A case study of the China-Pakistan Economic Corridor region. *Ecologic. Indic.* **2021**, *129*, 107955. [CrossRef]
19. Heike Hartmann, H.B. Trends in Extreme Precipitation Events in the Indus River Basin and Flooding in Pakistan. *Atmos. Ocean* **2013**, *52*, 77–91. [CrossRef]
20. Hussain, A.; Cao, J.; Hussain, I.; Begum, S.; Akhtar, M.; Wu, X.; Guan, Y.; Zhou, J. Observed Trends and Variability of Temperature and Precipitation and Their Global Teleconnections in the Upper Indus Basin, Hindukush-Karakoram-Himalaya. *Atmosphere* **2021**, *12*, 973. [CrossRef]
21. Adnan, S.; Ullah, K.; Gao, S.; Khosa, A.H.; Wang, Z. Shifting of agro-climatic zones, their drought vulnerability, and precipitation and temperature trends in Pakistan. *Int. J. Clim.* **2017**, *37*, 529–543. [CrossRef]
22. Gadiwala, M.S.; Burke, F. Climate change and precipitation in Pakistan—A meteorological prospect. *Int. J. Econ. Environ. Geol.* **2013**, *4*, 10–15.
23. Ahmad, I.; Tang, D.; Wang, T.; Wang, M.; Wagan, B. Precipitation trends over time using Mann-Kendall and spearman's rho tests in swat river basin, Pakistan. *Advan. Met.* **2015**, *2015*, 431860. [CrossRef]
24. Iqbal, M.F.; Athar, H. Variability, trends, and teleconnections of observed precipitation over Pakistan. *Theor. Appl. Clim.* **2018**, *134*, 613–632. [CrossRef]
25. Afzal, M.; Haroon, M.; Rana, A.; Imran, A. Influence of north Atlantic oscillations and southern oscillations on winter precipitation of northern Pakistan. *Pak. J. Meteorol.* **2013**, *9*, 18.
26. Iftikhar, A.; Zhaobo, R.A.; Weitao, D. Winter-Spring Precipitation Variability in Pakistan. *Am. J. Clim. Change* **2015**, *4*, 115.
27. Zaman, M.; Ahmad, I.; Usman, M.; Saifullah, M.; Anjum, M.N.; Khan, M.I.; Uzair Qamar, M. Event-Based Time Distribution Patterns, Return Levels, and Their Trends of Extreme Precipitation across Indus Basin. *Water* **2020**, *12*, 3373. [CrossRef]
28. Akhtar, M.; Zhao, Y.; Gao, G.; Gulzar, Q.; Hussain, A. Assessment of spatiotemporal variations of ecosystem service values and hotspots in a dryland: A case-study in Pakistan. *Land Degrad. Develop.* **2022**, *33*, 1383–1397. [CrossRef]
29. Nawaz, Z.; Li, X.; Chen, Y.; Guo, Y.; Wang, X.; Nawaz, N. Temporal and spatial characteristics of precipitation and temperature in Punjab, Pakistan. *Water* **2019**, *11*, 1916. [CrossRef]
30. Hussain, A.; Cao, J.; Ali, S.; Muhammad, S.; Ullah, W.; Hussain, I.; Akhtar, M.; Wu, X.; Guan, Y.; Zhou, J. Observed trends and variability of seasonal and annual precipitation in Pakistan during 1960–2016. *Int. J. Clim.* **2022**, *42*, 8313–8332. [CrossRef]
31. Bookhagen, B.; Burbank, D.W. Toward a complete Himalayan hydrological budget: Spatiotemporal distribution of snowmelt and rainfall and their impact on river discharge. *J. Geophy. Res. Earth Surf.* **2010**, *115*, 1–25. [CrossRef]
32. Abbas, A.; Ullah, S.; Ullah, W.; Waseem, M.; Dou, X.; Zhao, C.; Karim, A.; Zhu, J.; Hagan, D.F.T.; Bhatti, A.S. Evaluation and projection of precipitation in Pakistan using the Coupled Model Intercomparison Project Phase 6 model simulations. *Int. J. Clim.* **2022**, *42*, 6665–6684. [CrossRef]
33. Khan, I.; Waqas, T.; Ullah, S. Precipitation variability and its trend detection for monitoring of drought hazard in northern mountainous region of Pakistan. *Arab. J. Geosci.* **2020**, *13*, 698. [CrossRef]
34. Abbasi, A.M.; Shah, M.H.; Khan, M.A. Pakistan and Pakistani Himalayas. In *Wild Edible Vegetables of Lesser Himalayas*; Springer: Berlin/Heidelberg, Germany, 2015; pp. 1–18.
35. Black, M. *The Atlas of Water: Mapping the World's Most Critical Resource*; Univ of California Press: Berkeley, CA, USA, 2016.
36. Rondhi, M.; Fatikhul Khasan, A.; Mori, Y.; Kondo, T. Assessing the role of the perceived impact of climate change on national adaptation policy: The case of rice farming in Indonesia. *Land* **2019**, *8*, 81. [CrossRef]

37. Hussain, A.; Ali, H.; Begum, F.; Hussain, A.; Khan, M.Z.; Guan, Y.; Zhou, J.; Hussain, K. Mapping of Soil Properties under Different Land Uses in Lesser Karakoram Range, Pakistan. *Pol. J. Environ. Stud.* **2021**, *30*, 1181–1189. [CrossRef]
38. Azam, A.; Shafique, M. Agriculture in Pakistan and its Impact on Economy. A Review. *Inter. J. Adv. Sci. Technol.* **2017**, *103*, 47–60. [CrossRef]
39. Sharma, S.; Hamal, K.; Pokharel, B.; Fosu, B.; Wang, S.Y.S.; Gillies, R.R.; Aryal, D.; Shrestha, A.; Marahatta, S.; Hussain, A.; et al. Atypical forcing embedded in typical forcing leading to the extreme summer 2020 precipitation in Nepal. *Clim. Dyn.* **2023**, *10*, 1–12. [CrossRef]
40. Bhatti, A.S.; Wang, G.; Ullah, W.; Ullah, S.; Fiifi Tawia Hagan, D.; Kwesi Nooni, I.; Lou, D.; Ullah, I. Trend in extreme precipitation indices based on long term in situ precipitation records over Pakistan. *Water* **2020**, *12*, 797. [CrossRef]
41. Khalil, A. Inhomogeneity detection in the rainfall series for the Mae Klong River Basin, Thailand. *Appl. Water Sci.* **2021**, *11*, 147. [CrossRef]
42. Ahmed, K.; Nawaz, N.; Khan, N.; Rasheed, B.; Baloch, A. Inhomogeneity detection in the precipitation series: Case of arid province of Pakistan. *Environ. Develop. Sustain.* **2021**, *23*, 7176–7192. [CrossRef]
43. Ray, S.; Das, S.S.; Mishra, P.; Al Khatib, A.M.G. Time series SARIMA Modelling and forecasting of monthly rainfall and temperature in the south Asian countries. *Earth Syst. Environ.* **2021**, *5*, 531–546. [CrossRef]
44. Mirdashtvan, M.; Najafinejad, A.; Malekian, A.; Sa'doddin, A. Regional analysis of trend and non-stationarity of hydro-climatic time series in the Southern Alborz Region, Iran. *Int. J. Clim.* **2020**, *40*, 1979–1991. [CrossRef]
45. Piles, M.; Muñoz-Marí, J.; Guerrero-Curieses, A.; Camps-Valls, G.; Rojo-Álvarez, J.L. Autocorrelation Metrics to Estimate Soil Moisture Persistence from Satellite Time Series: Application to Semiarid Regions. *IEEE Tran. Geosci. Remote Sens.* **2021**, *60*, 4401417. [CrossRef]
46. Ullah, S.; You, Q.; Ali, A.; Ullah, W.; Jan, M.A.; Zhang, Y.; Xie, W.; Xie, X. Observed changes in maximum and minimum temperatures over China-Pakistan economic corridor during 1980–2016. *Atmos. Res.* **2019**, *216*, 37–51. [CrossRef]
47. Agbo, E.P.; Ekpo, C.M.; Edet, C.O. Analysis of the effects of meteorological parameters on radio refractivity, equivalent potential temperature and field strength via Mann-Kendall test. *Theor. Appl. Clim.* **2021**, *143*, 1437–1456. [CrossRef]
48. Ashraf, M.S.; Ahmad, I.; Khan, N.M.; Zhang, F.; Bilal, A.; Guo, J. Streamflow Variations in Monthly, Seasonal, Annual and Extreme Values Using Mann-Kendall, Spearmen's Rho and Innovative Trend Analysis. *Water. Res. Manag.* **2021**, *35*, 243–261. [CrossRef]
49. Karami, S.; Hossein Hamzeh, N.; Sabzezari, H.; Lo Alizadeh, M. Investigation of trend analysis of the number of dust stormy days and aerosol concentration derived from satellite in Khuzestan province by using non-parametric Mann-Kendall test. *J. Clim. Res.* **2021**, *1399*, 91–103.
50. Kubiak-Wójcicka, K.; Pilarska, A.; Kamiński, D. The Analysis of Long-Term Trends in the Meteorological and Hydrological Drought Occurrences Using Non-Parametric Methods—Case Study of the Catchment of the Upper Noteć River (Central Poland). *Atmosphere* **2021**, *12*, 1098. [CrossRef]
51. Ullah, S.; You, Q.; Ullah, W.; Ali, A. Observed changes in precipitation in China-Pakistan economic corridor during 1980–2016. *Atmos. Res.* **2018**, *210*, 1–14. [CrossRef]
52. Seenu, P.; Jayakumar, K. Comparative study of innovative trend analysis technique with Mann-Kendall tests for extreme rainfall. *Arab. J. Geosci.* **2021**, *14*, 536.
53. Mohsin, S.; Lone, M. Trend analysis of reference evapotranspiration and identification of responsible factors in the Jhelum River Basin, Western Himalayas. *Mod. Earth Syst. Environ.* **2021**, *7*, 523–535. [CrossRef]
54. Baig, M.R.I.; Naikoo, M.W.; Ansari, A.H.; Ahmad, S.; Rahman, A. Spatio-temporal analysis of precipitation pattern and trend using standardized precipitation index and Mann–Kendall test in coastal Andhra Pradesh. *Model. Earth. Syst. Environ.* **2021**, *8*, 2733–2752. [CrossRef]
55. Asgher, S.; Ahmad, M.; Kumar, N.; Kumari, M. Trend Analysis of Temperature and Rainfall using Mann Kendall Test and Sen's Slope Estimator in Bhaderwah Tehsil of Doda District. *Res. J. Agric. Sci.* **2021**, *12*, 1021–1026.
56. Aditya, F.; Gusmayanti, E.; Sudrajat, J. Rainfall trend analysis using Mann-Kendall and Sen's slope estimator test in West Kalimantan. In Proceedings of the IOP Conference Series: Earth and Environmental Science, Surakarta, Indonesia, 24–25 August 2021; p. 012006.
57. AlSubih, M.; Kumari, M.; Mallick, J.; Ramakrishnan, R.; Islam, S.; Singh, C.K. Time series trend analysis of rainfall in last five decades and its quantification in Aseer Region of Saudi Arabia. *Arab. J. Geosci.* **2021**, *14*, 519. [CrossRef]
58. Gupta, N.; Banerjee, A.; Gupta, S.K. Spatio-temporal trend analysis of climatic variables over Jharkhand, India. *Earth Syst. Environ.* **2021**, *5*, 71–86. [CrossRef]
59. Alsubih, M.; Mallick, J.; Talukdar, S.; Salam, R.; AlQadhi, S.; Fattah, M.A.; Thanh, N.V. An investigation of the short-term meteorological drought variability over Asir Region of Saudi Arabia. *Theor. Appl. Clim.* **2021**, *145*, 597–617. [CrossRef]
60. Chong, K.; Huang, Y.; Koo, C.; Ahmed, A.N.; El-Shafie, A. Spatiotemporal Variability Analysis of Standardized Precipitation Indexed Droughts Using Wavelet Transform. *J. Hydrol.* **2021**, *605*, 127299. [CrossRef]
61. Ullah, I.; Ma, X.; Yin, J.; Saleem, F.; Syed, S.; Omer, A.; Habtemicheal, B.A.; Liu, M.; Arshad, M. Observed changes in seasonal drought characteristics and their possible potential drivers over Pakistan. *Int. J. Clim.* **2021**, *42*, 1576–1596. [CrossRef]
62. Pandey, B.K.; Khare, D.; Tiwari, H.; Mishra, P.K. Analysis and visualization of meteorological extremes in humid subtropical regions. *Nat. Haz.* **2021**, *108*, 661–687. [CrossRef]

63. Sein, Z.M.M.; Zhi, X.; Ullah, I.; Azam, K.; Ngoma, H.; Saleem, F.; Xing, Y.; Iyakaremye, V.; Syed, S.; Hina, S. Recent variability of sub-seasonal monsoon precipitation and its potential drivers in Myanmar using in-situ observation during 1981–2020. *Int. J. Clim.* **2021**, *42*, 3341–3359. [CrossRef]
64. Ouyang, X.; Chen, D.; Zhou, S.; Zhang, R.; Yang, J.; Hu, G.; Dou, Y.; Liu, Q. A Slight Temperature Warming Trend Occurred over Lake Ontario from 2001 to 2018. *Land* **2021**, *10*, 1315. [CrossRef]
65. Hussain, A.; Cao, J.; Ali, S.; Ullah, W.; Muhammad, S.; Hussain, I.; Rezaei, A.; Hamal, K.; Akhtar, M.; Abbas, H. Variability in runoff and responses to land and oceanic parameters in the source region of the Indus River. *Ecologic. Indic.* **2022**, *140*, 109014. [CrossRef]
66. Yang, M.-S.; Hussain, I. Unsupervised Multi-View K-Means Clustering Algorithm. *IEEE Access* **2023**, *11*, 13574–13593. [CrossRef]
67. MacQueen, J. Some methods for classification and analysis of multivariate observations. In Proceedings of the Fifth Berkeley Symposium on Mathematical Statistics and Probability, Berkeley, CA, USA, 21 June–18 July 1967; pp. 281–297.
68. Shaheen, M.; ur Rehman, S.; Ghaffar, F. Correlation and congruence modulo based clustering technique and its application in energy classification. *Sustain. Comput. Infor. Syst.* **2021**, *30*, 100561. [CrossRef]
69. Hussain, A.; Cao, J.; Ali, S.; Ullah, W.; Muhammad, S.; Hussain, I.; Abbas, H.; Hamal, K.; Sharma, S.; Akhtar, M. Wavelet coherence of monsoon and large-scale climate variabilities with precipitation in Pakistan. *Int. J. Clim.* **2022**, *42*, 9950–9966. [CrossRef]
70. Ikuemonisan, F.E.; Ozebo, V.C.; Olatinsu, O.B. Investigation of Sentinel-1-derived land subsidence using wavelet tools and triple exponential smoothing algorithm in Lagos, Nigeria. *Environ. Earth Sci.* **2021**, *80*, 722. [CrossRef]
71. He, L.; Freudenreich, T.; Yu, W.; Pelowski, M.; Liu, T. Methodological structure for future consumer neuroscience research. *Psy. Mark.* **2021**, *38*, 1161–1181. [CrossRef]
72. Vacha, L.; Barunik, J. Co-movement of energy commodities revisited: Evidence from wavelet coherence analysis. *Energy Econ.* **2012**, *34*, 241–247. [CrossRef]
73. Grinsted, A.; Moore, J.C.; Jevrejeva, S. Application of the cross wavelet transform and wavelet coherence to geophysical time series. *Nonlinear Process. Geophys.* **2004**, *11*, 561–566. [CrossRef]
74. Baudouin, J.-P.; Herzog, M.; Petrie, C.A. Cross-validating precipitation datasets in the Indus River basin. *Hyd. Earth Syst. Sci.* **2020**, *24*, 427–450. [CrossRef]
75. Gottschalck, J.; Meng, J.; Rodell, M.; Houser, P. Analysis of multiple precipitation products and preliminary assessment of their impact on global land data assimilation system land surface states. *J. Hydromet.* **2005**, *6*, 573–598. [CrossRef]
76. Safdar, F.; Khokhar, M.F.; Mahmood, F.; Khan, M.Z.A.; Arshad, M. Observed and predicted precipitation variability across Pakistan with special focus on winter and pre-monsoon precipitation. *Environ. Sci. Pollut. Res.* **2022**, *30*, 4510–4530. [CrossRef] [PubMed]
77. Hussain, A.; Ali, S.; Begum, S.; Hussain, I.; Ali, H. Climate Change Perspective in Mountain Area: Impacts and Adaptations in Naltar Valley, Western Himalaya, Pakistan. *Fresenius Environ. Bull.* **2019**, *28*, 6683–6691.
78. Latif, M.; Syed, F.; Hannachi, A. Rainfall trends in the South Asian summer monsoon and its related large-scale dynamics with focus over Pakistan. *Clim. Dyn.* **2017**, *48*, 3565–3581. [CrossRef]
79. Islam, T.; Md, A.R.; Rahman, M.; Khatun, R.; Hu, Z. Spatiotemporal trends in the frequency of daily rainfall in Bangladesh during 1975–2017. *Theor. Appl. Clim.* **2020**, *141*, 869–887. [CrossRef]
80. Yaseen, M.; Ahmad, I.; Guo, J.; Azam, M.I.; Latif, Y. Spatiotemporal Variability in the Hydrometeorological Time-Series over Upper Indus River Basin of Pakistan. *Adv. Meteor.* **2020**, *2020*, 5852760. [CrossRef]
81. Ahmed, K.; Shahid, S.; Chung, E.-S.; Ismail, T.; Wang, X.-J. Spatial distribution of secular trends in annual and seasonal precipitation over Pakistan. *Clim. Res.* **2017**, *74*, 95–107. [CrossRef]
82. Hanif, M.; Khan, A.H.; Adnan, S. Latitudinal precipitation characteristics and trends in Pakistan. *J. Hydrol.* **2013**, *492*, 266–272. [CrossRef]
83. Ullah, W.; Wang, G.; Lou, D.; Ullah, S.; Bhatti, A.S.; Ullah, S.; Karim, A.; Hagan, D.F.T.; Ali, G. Large-scale atmospheric circulation patterns associated with extreme monsoon precipitation in Pakistan during 1981–2018. *Atmos. Res.* **2021**, *253*, 105489. [CrossRef]
84. Niyogi, D.; Kishtawal, C.; Tripathi, S.; Govindaraju, R.S. Observational evidence that agricultural intensification and land use change may be reducing the Indian summer monsoon rainfall. *Water Resour. Res.* **2010**, *46*, 1–17. [CrossRef]
85. Priya, P.; Mujumdar, M.; Sabin, T.; Terray, P.; Krishnan, R. Impacts of Indo-Pacific sea surface temperature anomalies on the summer monsoon circulation and heavy precipitation over northwest India–Pakistan region during 2010. *J. Clim.* **2015**, *28*, 3714–3730. [CrossRef]
86. Ahmad, I.; Zhang, F.; Tayyab, M.; Anjum, M.N.; Zaman, M.; Liu, J.; Farid, H.U.; Saddique, Q. Spatiotemporal analysis of precipitation variability in annual, seasonal and extreme values over upper Indus River basin. *Atmos. Res.* **2018**, *213*, 346–360. [CrossRef]
87. Hasson, S. Future water availability from Hindukush-Karakoram-Himalaya Upper Indus Basin under conflicting climate change scenarios. *Climate* **2016**, *4*, 40. [CrossRef]
88. Hasson, S.; Lucarini, V.; Khan, M.R.; Petitta, M.; Bolch, T.; Gioli, G. Early 21st century snow cover state over the western river basins of the Indus River system. *Hydrol. Earth Syst. Sci.* **2014**, *18*, 4077–4100. [CrossRef]
89. Bocchiola, D.; Diolaiuti, G. Recent (1980–2009) evidence of climate change in the upper Karakoram, Pakistan. *Theor. Appl. Clim.* **2013**, *113*, 611–641. [CrossRef]
90. Ali, N.; Ahmad, I.; Chaudhry, A.; Raza, M. Trend analysis of precipitation data in Pakistan. *Sci. Int.* **2015**, *27*, 803–808.

91. Iqbal, Z.; Shahid, S.; Ahmed, K.; Ismail, T.; Nawaz, N. Spatial distribution of the trends in precipitation and precipitation extremes in the sub-Himalayan region of Pakistan. *Theor. Appl. Clim.* **2019**, *137*, 2755–2769. [CrossRef]
92. Ahmad, W.; Fatima, A.; Awan, U.K.; Anwar, A. Analysis of long term meteorological trends in the middle and lower Indus Basin of Pakistan—A non-parametric statistical approach. *Glob. Planet. Chang.* **2014**, *122*, 282–291. [CrossRef]
93. Guo, X.; Wang, L.; Tian, L. Spatio-temporal variability of vertical gradients of major meteorological observations around the Tibetan Plateau. *Int. J. Clim.* **2016**, *36*, 1901–1916. [CrossRef]
94. Li, Z.; He, Y.; Wang, C.; Wang, X.; Xin, H.; Zhang, W.; Cao, W. Spatial and temporal trends of temperature and precipitation during 1960–2008 at the Hengduan Mountains, China. *Quat. Int.* **2011**, *236*, 127–142. [CrossRef]
95. Hussain, M.S.; Lee, S. The regional and the seasonal variability of extreme precipitation trends in Pakistan. *Asia Pac. J. Atmos. Sci.* **2013**, *49*, 421–441. [CrossRef]
96. Zhou, L.; Zhu, J.; Zou, H.; Ma, S.; Li, P.; Zhang, Y.; Huo, C. Atmospheric moisture distribution and transport over the Tibetan Plateau and the impacts of the South Asian summer monsoon. *Act. Meteor. Sin.* **2013**, *27*, 819–831. [CrossRef]
97. Zhang, R.; Jiang, D.; Zhang, Z.; Yu, E. The impact of regional uplift of the Tibetan Plateau on the Asian monsoon climate. *Palaeogeogr. Palaeoclimatol. Palaeoecol.* **2015**, *417*, 137–150. [CrossRef]
98. Hasson, S.; Böhner, J.; Lucarini, V. Prevailing climatic trends and runoff response from Hindukush–Karakoram–Himalaya, upper Indus Basin. *Earth Syst. Dyn.* **2017**, *8*, 337–355. [CrossRef]
99. Ullah, S.; You, Q.; Wang, G.; Ullah, W.; Sachindra, D.; Yan, Y.; Bhatti, A.S.; Abbas, A.; Jan, M.A. Characteristics of human thermal stress in South Asia during 1981–2019. *Environ. Res. Lett.* **2022**, *17*, 104018. [CrossRef]
100. De Oliveira-Júnior, J.F.; Shah, M.; Abbas, A.; Iqbal, M.S.; Shahzad, R.; de Gois, G.; da Silva, M.V.; da Rosa Ferraz Jardim, A.M.; de Souza, A. Spatiotemporal analysis of drought and rainfall in Pakistan via Standardized Precipitation Index: Homogeneous regions, trend, wavelet, and influence of El Niño-southern oscillation. *Theor. Appl. Clim.* **2022**, *149*, 843–862. [CrossRef]
101. Attada, R.; Dasari, H.P.; Chowdary, J.S.; Yadav, R.K.; Knio, O.; Hoteit, I. Surface air temperature variability over the Arabian Peninsula and its links to circulation patterns. *Int. J. Clim.* **2019**, *39*, 445–464. [CrossRef]
102. De Beurs, K.M.; Henebry, G.M.; Owsley, B.C.; Sokolik, I.N. Large scale climate oscillation impacts on temperature, precipitation and land surface phenology in Central Asia. *Environ. Res. Lett.* **2018**, *13*, 065018. [CrossRef]
103. Syed, F.S.; Giorgi, F.; Pal, J.; Keay, K. Regional climate model simulation of winter climate over Central–Southwest Asia, with emphasis on NAO and ENSO effects. *Int. J. Clim.* **2010**, *30*, 220–235. [CrossRef]